ISSN 1070-3632, Russian Journal of General Chemistry, 2007, Vol. 77, No. 3, pp. 336–342. © Pleiades Publishing, Ltd., 2007.
Original Russian Text © V.K. Krut'ko, A.I. Kulak, L.A. Lesnikovich, I.V. Trofimova, O.N. Musskaya, G.K. Zhavnerko, I.V. Paribok, 2007, published in Zhurnal Obshchei Khimii, 2007, Vol. 77, No. 3, pp. 366–373.

Influence of the Dehydration Procedure on the Physicochemical Properties of Nanocrystalline Hydroxylapatite Xerogel

V. K. Krut'ko[a], A. I. Kulak[a], L. A. Lesnikovich[a], I. V. Trofimova[a], O. N. Musskaya[a], G. K. Zhavnerko[b], and I. V. Paribok[b]

[a] *Institute of General and Inorganic Chemistry, National Academy of Sciences of Belarus, ul. Surganova 9, Minsk, 220072 Belarus*
e-mail: tsuber@igic.bas-net.by

[b] *Institute of Chemistry of New Materials, National Academy of Sciences of Belarus, Minsk, Belarus*

Received November 28, 2006

Abstract—The influence of various dehydration procedures on the physicochemical properties of hydroxylapatite gel was examined. The best dehydration procedure is freezing, leading to the formation of a nanocrystalline hydroxylapatite powder without intermediate formation of a monolithic xerogel. Examination by the layer self-arrangement method, scanning electron microscopy, and atomic-force microscopy showed that the powder particles are spherical aggregates from 0.4 to 2.0 μm in size, consisting of nanoparticles 16–30 nm in diameter.

DOI: 10.1134/S1070363207030036

Calcium hydroxophosphate $Ca_{10}(PO_4)_6(OH)_2$, also termed hydroxylapatite, is the main inorganic component of bone and tooth tissues [1–3]. Bioceramic materials based on hydroxylapatite, when used as artificial bone analogs, have certain advantages over natural grafts, because they do not cause immune rejection, enhance to a greater extent the proliferative activity of osteoblasts, and stimulate reparative osteogenesis at the grafting site; they also suppress inflammation in the bone wound [4]. These factors make synthetic hydroxylapatite promising for the development of biocompatible materials for oral surgery, stomatology, orthopedy, ophthalmology, and also for therapy and prevention of osteoporosis [5–7]. It is important that the properties of synthetic hydroxylapatite and bioinorganic materials based on it are largely determined by the preparation conditions, composition and concentration of impurities, features of pore structure, etc. In view of the fact that the gel form of hydroxylapatite is the most biologically active [8], our goal was to study its physicochemical properties and particle morphology, and also to examine the effect of various procedures of water removal on the final product, with the subsequent formation of a monolithic xerogel, powder, or ceramics.

In centrifugation of a hydroxylapatite gel, with an increase in the rotation rate and centrifugation time, the amount of the xerogel formed upon subsequent drying at 95°C to constant weight increases from 6.2 to 28.2 wt %, and the amount of water removed during drying correspondingly decreases (Table 1). The subsequent heat treatment at 800°C for 4 h leads to an insignificant weight loss of the hydroxylapatite dried at 95°C: The amount of the xerogel decreases from 6.2–28.2 to 5.8–26.0 wt %, i.e., additional 0.4–2.2% of water is removed; that is, the major portion of water is removed from the hydroxylapatite gel at 95°C. This conclusion is consistent with the results of thermal analysis, X-ray diffraction, and IR spectroscopy.

To find the best procedure for dehydration of hydroxylapatite gel, we examined the effect of various drying procedures and of low temperatures on its properties (Table 2). Depending on the drying procedure, either a monolithic xerogel or a powder can be obtained; drying of hydroxylapatite gel in air at 40–60°C to constant weight leads to the formation of a monolithic xerogel in the form of dense conglomerates of irregular shape, which can be ground mechanically to a powder with a particle size ≤60 μm and specific surface area of 170–180 $m^2 g^{-1}$.

To obtain a finely dispersed powder with increased friability without mechanical grinding of the xerogel, it is efficient to use dehydrating solvents (alcohol, acetone) in the stage of precipitate separation from the mother liquor.

Freeze drying of hydroxylapatite gel gives a powder consisting of coarse porous particles (conglomer-

Table 1. Amount of water removed from hydroxylapatite xerogel in the course of centrifugation, drying, and heat

Centrifugation conditions		Drying at 95°C		Heat treatment at 800°C	
treatment rate, rpm	time, min	H_2O, wt %	hydroxylapatite gel, wt %	H_2O, wt %	hydroxylapatite gel, wt %
0	0	93.8	6.2	94.2	5.8
1000	5	91.9	8.1	92.5	7.5
	10	91.3	8.7	91.9	8.1
	15	88.8	11.2	89.5	10.5
2000	5	86.4	13.6	87.5	12.5
	10	86.1	13.9	87.1	12.9
	15	85.5	14.5	86.6	13.4
3000	15	88.3	11.7	89.2	10.8
12000	30	71.8	28.2	74.0	26.0

Table 2. Physicochemical properties of synthetic hydroxylapatite

Procedure for water removal from hydroxylapatite gel	Crystallite size, nm	Specific surface area, $m^2\ g^{-1}$	Bulk density, $g\ cm^{-3}$
	Nanocrystalline hydroxylapatite		
Drying in air (60°C)	7.3	175	0.68
	8.9	181	0.52
Drying with alcohol	6.9	168	0.66
	7.8	170	0.62
	8.8	180	0.53
Freeze drying	8.3	183	0.47
	9.6	199	0.40
	9.7	248	0.31
Freezing (–18 and –196°C)	9.8	90	0.50
	8.6	109	0.48
	Polycrystalline hydroxylapatite		
Heat treatment (800 and 1300°C)	90	14–25	0.70
	100	1–3	0.68

ates) 300 to 1000 μm in size, with a large specific surface area (about 200–250 $m^2\ g^{-1}$).

Freezing of the centrifuged (2000 rpm, 15 min) hydroxylapatite gel at –18°C for 2 days allows separation of 53 wt % of water relative to the gel before centrifugation; after drying in air at 60°C for 1 day, an additional ~30 wt % of water is removed. Thus, the total amount of water removed from the hydroxylapatite gel is 83 wt %. The resulting precipitate is a coarsely dispersed powder with conglomerates of irregular shape and size of 3–6 mm, with the specific surface area of 90–98 $m^2\ g^{-1}$. To prepare a finely dispersed powder, the hydroxylapatite gel should be subjected to ultrasonic treatment before freezing at –18°C for 1 day. When a centrifuged (2000 rpm, 15 min) hydroxylapatite gel is frozen with liquid nitrogen (at –196°C), complete freezing takes 10–20 min. The largest amount of water (84–87 wt %) is separated after thawing and drying in air at 135°C; in so doing, a finely dispersed hydroxylapatite powder is formed, similar in external appearance to the freeze-dried powder with a specific surface area of 100–109 $m^2\ g^{-1}$. Hence, freezing is a convenient procedure for quick and fairly complete separation of water from hydroxylapatite gel with the formation of a finely dispersed powder that does not require additional grinding.

X-ray phase analysis of hydroxylapatite dried in air at 60°C and frozen with the subsequent drying under the same conditions revealed the characteristic hy-

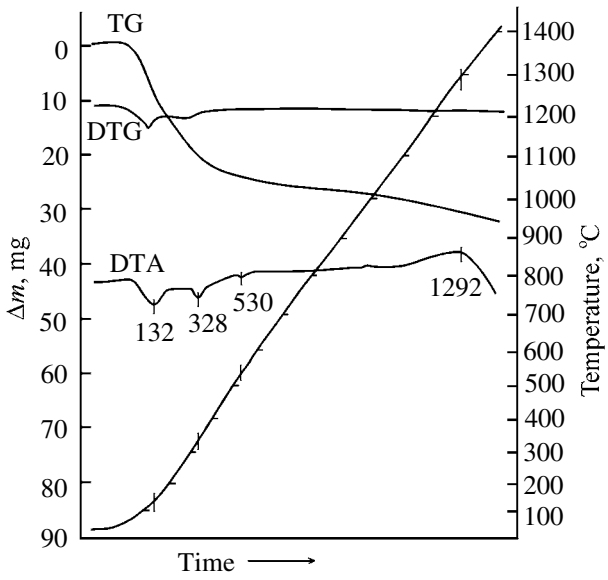

Fig. 1. Derivatogram of hydroxylapatite powder.

droxylapatite reflections, identical for both samples. Thus, freezing only weakly affects the crystal structure of hydroxylapatite but distorts the colloidal structure of the gel, which decreases the precipitate volume and makes its particles coarser (up to ~1 μm in size). A similar result is attained by boiling of a hydroxylapatite precipitate in the mother liquid, which leads, according to atomic-force microscopy, to a decrease in the precipitate volume and to particle coarsening.

Heat treatment at 800 and 1300°C of the hydroxylapatite powder after its grinding and drying in air at 60°C leads to a considerable increase in the crystallite size and to a decrease in the specific surface area from 14–25 to 1–3 $m^2 g^{-1}$, respectively (Table 2).

According to the DTA data for hydroxylapatite powder dried in air at 60°C to constant weight, dehydration occurs in three steps (Fig. 1). Removal of approximately a half of water of crystallization occurs in the range of pronounced endothermic effect with a minimum at 132°C. The remaining water is gradually removed in the temperature range 328–530°C, and the DTG curve flattens out, which, in combination with the X-ray diffraction data (Fig. 2a), is indicative of gradual crystallization of a single-phase product. The loss of water of crystallization was accompanied by transformation of nanocrystalline hydroxylapatite into polycrystalline hydroxylapatite and by an increase in the crystallite size from 7–10 to 90–100 nm (Table 2), which is confirmed by X-ray diffraction. The diffraction patterns of hydroxylapatite samples heat-treated at various temperatures show no evidence of the appearance of new modifications with increasing temperature; the structure merely becomes more perfect.

In the IR spectra of hydroxylapatite (Fig. 2b), bands at 500–630 cm^{-1} are due to bending vibrations of the PO_4 tetrahedra, overlapping with the stretching vibrations of the Ca–O bonds, and the bands at 900–1100 cm^{-1}, due to P–O stretching vibrations (Table 3). The bending vibrations of water molecules of hydration give a single band at 1636 cm^{-1}; the stretching vibrations of OH groups give a broad structureless band in the range 3000–3600 cm^{-1}, suggesting the presence of a system of hydrogen bonds. A narrow

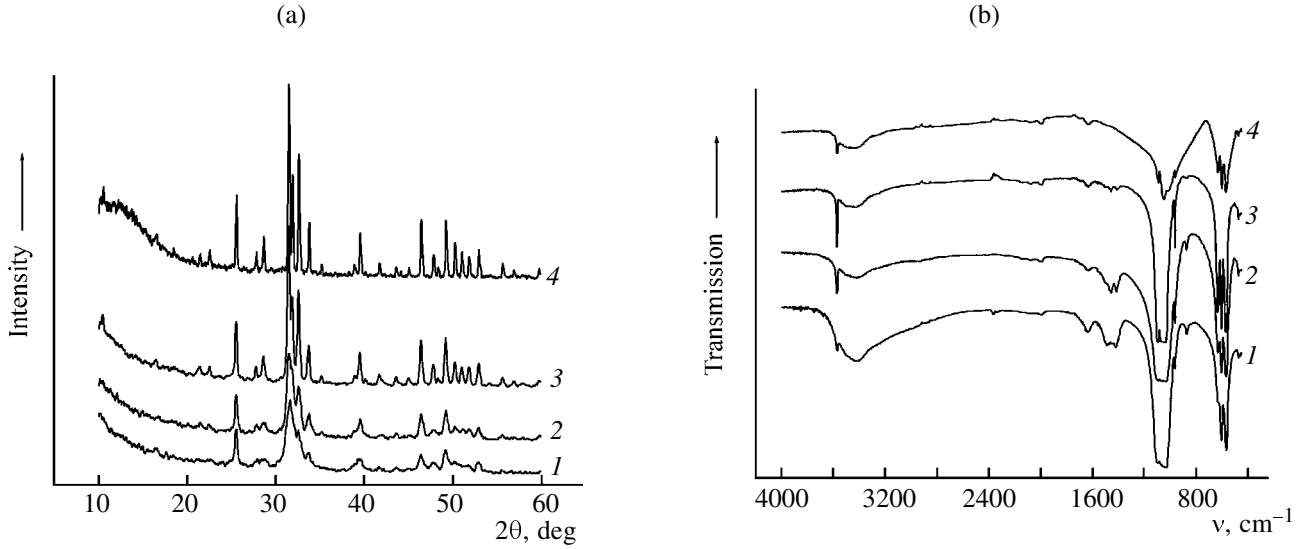

Fig. 2. (a) X-ray diffraction patterns and (b) IR spectra of hydroxylapatite: (*1*) 60°C, 1 day; (*2*) 600°C, 4 h; (*3*) 800°C, 3 h; and (*4*) 1300°C, 1 h.

Table 3. Wavenumbers (cm^{-1}) and assignments of absorption bands in the IR spectra of hydroxylapatite

Temperature and time of heating of hydroxylapatite samples				Hydroxylapatite reference [9]	Assignment
60°C, 1 day	600°C, 4 h	800°C, 3 h	1300°C, 1 h		
565	567	570	572	570	$\delta(PO_4^{3-})$
604	603	603	601	601	
–	631	632	631	631	
873	874	–	–	–	$\delta(CO_3^{2-})$
962	962	963	961	960	ν(P–O)
1032	1031	1040	1045	1045	
1094	1094	1092	1090	1090	
1419	1414	–	–	–	$\delta(CO_3^{2-})$
1636	1636	–	–	–	δ(OH)
3418	3420	3430	3428	3430	ν(OH)
3569	3572	3572	3570	3570	

band at 3572 cm^{-1} observed against the background of this broad band is characteristic of OH groups that are coordinated by a cation and are not involved in hydrogen bonding (structural OH groups).

The IR spectra show that, with an increase in the heat treatment temperature from 600 to 1300°C (Fig. 2b), the hydrogen bonds are broken and water of crystallization is removed. The extent of resolution and the intensity of absorption bands, especially in the range of stretching vibrations of PO_4 tetrahedra, appreciably increases with temperature, which, in agreement with the X-ray diffraction data, suggests an increase in the degree of crystallinity. Furthermore, samples heated at 200°C for 6 h, at 400°C for 5 h, and at 600°C for 4 h have an IR spectrum similar to that of the samples dried at 60°C for 1 day.

Pressing at 39.2 MPa of finely dispersed powders of both nanocrystalline and polycrystalline hydroxylapatite with a particle size of up to 63 μm, followed by heat treatment at 1300°C for 1 h, yields a strong hydroxylapatite ceramics with a microhardness of about 5 GPa at a load of 50 g. Compaction of the powder of nanocrystalline hydroxylapatite, as a rule, does not alter the initial particle shape (Fig. 3a), but their size decreases to 7.5–14.3 μm, probably due to shrinkage caused mainly by removal of water of crystallization in the course of high-temperature annealing; bridges arise between particles, and a pronounced coarsely porous structure is formed. The powder of polycrystalline hydroxylapatite is compacted in a somewhat different manner (Fig. 3b): The particles lose their initial shape, their size decreases to 7.5–12.8 μm, and the pores are filled with fine particles 0.8–2.3 μm in size.

In the course of layer self-arrangement, particles of hydroxylapatite gel are deposited as a monolayer onto silicon supports with a positive polyelectrolytic sublayer, PDDA/PSS/PDDA (see Experimental), which indicates that particles of the hydroxylapatite gel bear a negative charge. Electron-microscopic (SEM) examination of hydroxylapatite gel showed that it consists of aggregated particles of regular spherical shape and

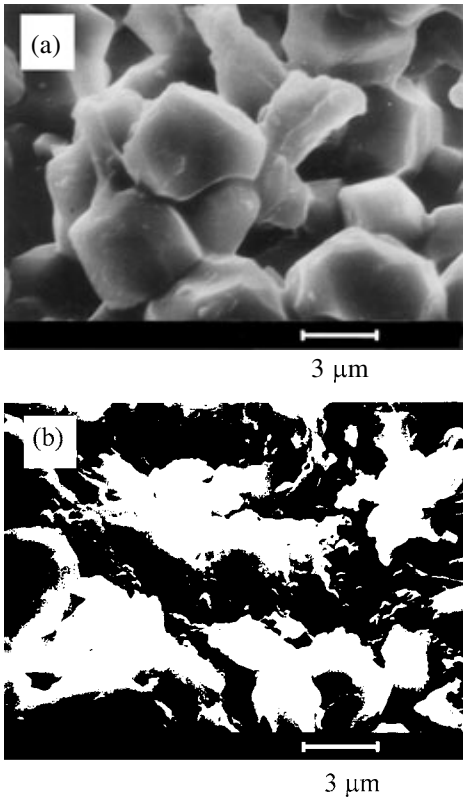

Fig. 3. SEM patterns of compacted hydroxylapatite powder: (a) nanocrystalline and (b) polycrystalline.

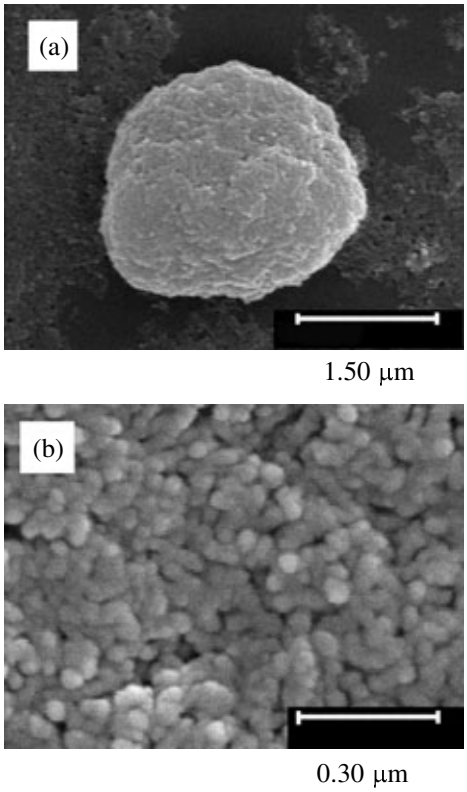

Fig. 4. SEM patterns of hydroxylapatite particles (Figs. 4a and 4b differ in magnification).

size of 2 μm (Fig. 4a), which, in turn, consist of nanoparticles from 16 to 30 nm in diameter (Fig. 4b).

To confirm these results, we examined by atomic-force microscopy (AFM) in the contact mode the following specimens of hydroxylapatite gel: (1) freshly precipitated, not washed, pH 10.6; (2) "mature," washed to pH 7.0; (3) stored for 1 year, pH 7.0; and (4) boiled and centrifuged (2000 rpm, 15 min), pH 7.6. Figure 5 shows the surface topography and friction data and the corresponding 3D AFM patterns.

The morphology of freshly precipitated hydroxylapatite gel is represented by nonuniform distribution of coarse and fine particles (Fig. 5a) with clear boundaries; aggregate clustering have not yet occurred. The washed "mature" hydroxylapatite gel consists of spherical aggregates with indefinite boundaries, which form clusters (Fig. 5b). The washed hydroxylapatite gel stored for a year (Fig. 5c) or boiled (Fig. 5d) consists of clusters of aggregated particles with the largest aggregate size.

Comparison of the AFM patterns of various hydroxylapatite specimens shows that the particle morphology is the same in all the cases, i.e., the particles are spherical aggregates consisting of nanoparticles. The mean size of aggregated particles ranges from 120–380 nm to 2 μm. Prolonged storage and boiling of hydroxylapatite gel result in particle coarsening, up to formation of large agglomerates.

It should be noted in conclusion that centrifugation allows preparation of hydroxylapatite gel of the required moisture content and viscosity with the dry matter content of 74.0–89.5 wt %, and freezing allows separation of the largest amount of water from the gel, with the subsequent formation of finely dispersed nanocrystalline powder. Depending on the gel dehydration procedure, the following materials are obtained: (1) monolithic xerogel; (2) finely dispersed powder with a conglomerate size of up to 60 μm and specific surface area of 180–200 $m^2 g^{-1}$; (3) freeze-dried powder with a conglomerate size of 300–1000 μm and specific surface area of 200–250 $m^2 g^{-1}$; and (4) strong hydroxylapatite ceramics. Examination by scanning electron and atomic-force microscopy with layer self-arrangement of particles on the surface of silicon substrates showed that the dried hydroxylapatite gel consists of aggregated spherical particles of the size from 400 nm to 2 μm, which, in turn, consist of nanoparticles 16–30 nm in diameter.

EXPERIMENTAL

Hydroxylapatite gel was prepared by the reaction of aqueous solutions of $CaCl_2$ and $(NH_2)_2HPO_4$ at a Ca/P ratio of 1.67 in the presence of concentrated ammonia at pH 10–11, in accordance with the procedure we developed previously [10, 11]. In the course of the synthesis, an amorphous phase of the composition $Ca_{10-x}(HPO_4)_x(PO_4)_{6-x}(OH)_{2-x}$ $(0 < x < 2)$ precipitated; within 7–10 days, it hydrolytically transformed into a stable hydroxylapatite gel, which was washed with distilled water to pH 7.0–7.4.

The hydroxylapatite gel was separated on an LU-411 centrifuge (Hungary) at 1000 to 2000 rpm for 5–30 min. The freezing was performed at –18°C (in a freezer) or at –196°C (in liquid nitrogen); prior to freezing, some samples were ultrasonically treated on a UZD 3-20 ultrasonic disintegrator in the continuous and pulse modes at 44 kHz for 5 min. The hydroxylapatite gel was dehydrated by heat treatment at 60–135°C, freeze drying, or treatment with dehydrating agents (alcohol, acetone). The specific surface area of hydroxylapatite was determined by the Klyachko–Gurvich prompt method from nitrogen adsorption. Thermal analysis was performed with an OD-103 MOM derivatograph with an open thermoceramic crucible in the range 17–1500°C at a heating rate of 7.5 deg min^{-1}. X-ray phase analysis was performed with a DRON-3 diffractometer (CuK_α radiation, λ

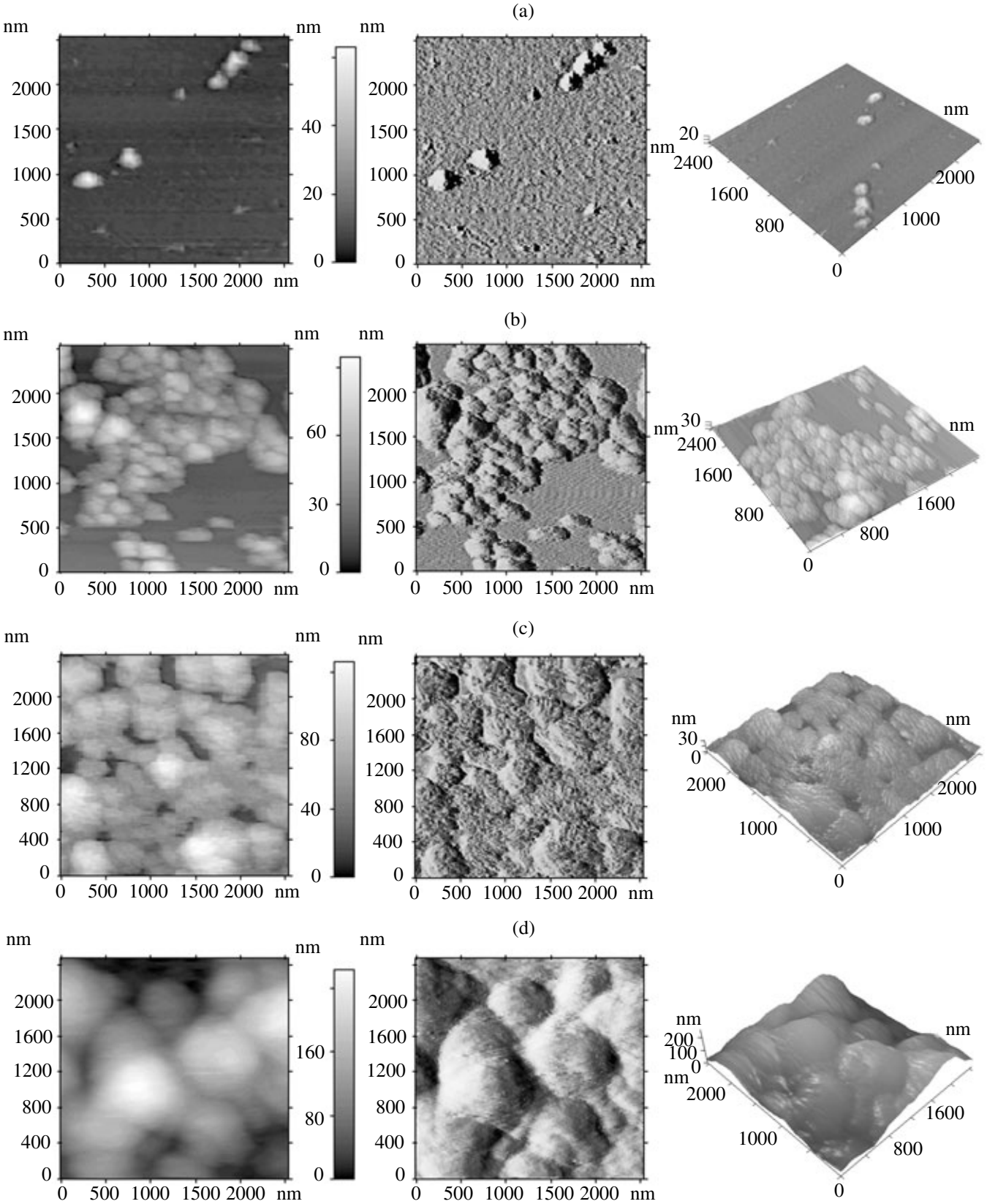

Fig. 5. AFM patterns of hydroxylapatite particles: (a) freshly precipitated, pH 10.6; (b) "mature," washed to pH 7.0; (c) stored for 1 year, pH 7.0; and (d) boiled and centrifuged (2000 rpm, 15 min), pH 7.6.

1.5405 Å); the diffraction patterns were processed with POWDER X software. The IR spectra were recorded on a Midac 2000 FTIR spectrometer using KBr pellets.

Morphological characteristics of hydroxylapatite gel particles were determined by scanning electron microscopy on a Hitachi S-806 microscope and by atomic-force microscopy on a Femtoscan-001 microscope in combination with the layer self-arrangement method [12, 13]. For this purpose, silicon supports were cleaned for 10–15 min with a boiling 1 : 1 mixture of H_2SO_4 and HNO_3, after which they were hydrophilized in an aqueous solution of 9% NH_3 and 3% H_2O_2 at 50–60°C for 10 min. Then the support surface was modified with alternating polyelectrolyte layers (3–4 layers): positively charged poly(diallyldimethylammonium chloride) (PDDA, M_2 200000–350000) and negatively charged sodium polystyrenesulfonate (PSS, M_w 70000). The PDDA solution was prepared in 0.5 M NaCl, and the PSS solution, in water. After the formation of a polyelectrolyte sublayer, PDDA/PSS/PDDA or PDDA/PSS/PDDA/PSS, the surface acquired a positive or negative charge, and then the supports were treated with a strongly diluted hydroxylapatite gel for 20 min.

The SEM patterns were obtained at ×20000 and ×100000 magnifications. AFM patterns were obtained in the contact mode using standard cantilevers 100 and 200 μm long with a Si_3N_4 needle (elastic constant 0.06, 0.12, and 0.36 N m^{-1}). The scanning rate was chosen in the range 1–5 Hz, and the information density was 512 × 512 dots. The needle force acting on the specimen in the course of scanning did not exceed 1–5 nN.

ACKNOWLEDGMENTS

The study was financially supported by the State Integrated Program of Scientific Research "Nanomaterials and Nanotechnologies" (task no. 5.06.02) and by the Belarussian Republican Foundation for Basic Research (project no. Kh06-023).

REFERENCES

1. Barinov, S.M. and Komlev, V.S., *Biokeramika na osnove fosfatov kal'tsiya* (Bioceramics Based on Calcium Phosphates), Moscow: Nauka, 2005.
2. Tret'yakov, Yu.D., *Usp. Khim.,* 2004, vol. 73, no. 9, p. 899.
3. Orlovskii, V.P., Kurdyumov, S.G., and Slivka, O.I., *Stomatologiya,* 1996, no. 5, p. 68.
4. Kulak, A.I., Lesnikovich, L.A., Trofimova, I.V., et al., *Izv. Bel. Inzh. Akad.,* 1997, no. 1(3), p. 31.
5. Suchanek, W. and Yoshimura, M., *J. Mater. Res.,* 1998, vol. 13, no. 1, p. 94.
6. Orlovskii, V.P., Komlev, V.S., and Barinov, S.M., *Neorg. Mater.,* 2002, vol. 38, no. 10, p. 1159.
7. Lesnikovich, L.A., Tsuber, V.K., Trofimova, I.V., et al., *Nauka Innov. Nats. Akad. Nauk Bel.,* 2003, nos. 5–6, p. 75.
8. Tsuber, V.K., Lesnikovich, L.A., Trofimova, I.V., et al., *Vestsi Nats. Akad. Navuk Bel., Ser. Khim. Navuk,* 2004, no. 1, p. 37.
9. Zharskii, I.M., Vorob'ev, N.I., Mel'nikova, R.Ya., et al., *Svoistva i metody identifikatsii veshchestv v neorganicheskoi tekhnologii* (Properties and Methods for Identification of Substances in Inorganic Technology), Minsk: FFI, 1996.
10. Belarussian Patent 2302, 1998.
11. Lesnikovich, L.A., Trofimova, I.V., Il'yushchenko, A.F., et al., *Vestsi Nats. Akad. Navuk Bel., Ser. Khim. Navuk,* 1999, no. 1, p. 15.
12. Hoogeveen, N.G., Boehmer, M.A.C., Fleer, G.J., et al., *Langmuir,* 1996, vol. 12, p. 3675.
13. Castelnovo, M. and Joanny, J.-F., *Langmuir,* 2000, vol. 16, p. 7524.